Biochimica et Biophysica Acta 1850 (2015) 681–690

Contents lists available at ScienceDirect

Biochimica et Biophysica Acta

journal homepage: www.elsevier.com/locate/bbagen

Changes to both cardiac metabolism and performance accompany acute reductions in functional capillary supply

David Hauton [a,*], James Winter [b], Abdullah A. Al-Shammari [c,d], Eamonn A. Gaffney [c], Rhys D. Evans [e], Stuart Egginton [f]

[a] School of Food Science and Nutrition, University of Leeds, Woodhouse Lane, Leeds LS2 9JT, United Kingdom
[b] Cardiovascular Physiology, The Rayne Institute, King's College London, London SE1 7EH, United Kingdom
[c] Mathematical Institute, University of Oxford, Woodstock Road, Oxford OX2 6GG, United Kingdom
[d] Department of Mathematics, Faculty of Sciences, Kuwait University, P.O. Box 5969, Khaldiya 13060, Kuwait
[e] Department of Physiology, Anatomy and Genetics, Sherrington Building, University of Oxford, South Parks Road, Oxford OX1 3PT, United Kingdom
[f] School of Biomedical Sciences, University of Leeds, Clarendon Way, Leeds LS2 9JT, United Kingdom

ARTICLE INFO

Article history:
Received 25 June 2014
Received in revised form 14 November 2014
Accepted 12 December 2014
Available online 18 December 2014

Keywords:
Working heart
Microspheres
Cardiac performance
Metabolism
Arteriole occlusion
Capillary domain

ABSTRACT

Background: The relative importance of arteriole supply or ability to switch between substrates to preserve cardiac performance is currently unclear, but may be critically important in conditions such as diabetes.
Methods: Metabolism of substrates was measured before and after infusion of polystyrene microspheres in the perfused working heart to mimic random capillary loss due to microvascular disease. The effect of acute loss of functional capillary supply on palmitate and glucose metabolism together with function was quantified, and theoretical tissue oxygen distribution calculated from histological samples and ventricular VO_2 estimated.
Results: Microsphere infusion led to a dose-dependent decrease in rate-pressure product (RPP) and oxygen consumption ($P < 0.001$). Microsphere infusion also increased work/unit oxygen consumption of hearts ('efficiency') by 25% ($P < 0.01$). When corrected for cardiac work palmitate oxidation remained tightly coupled to very low workloads (RPP < 2500 mm Hg/min), illustrating a high degree of metabolic control. Arteriole occlusion by microspheres decreased the density of patent capillaries ($P < 0.001$) and correspondingly increased the average capillary supply area by 40% ($P < 0.01$). Calculated rates of oxygen consumption declined from 16.6 ± 7.2 ml/100 ml/min to 12.4 ± 9 ml/100 ml/min following arteriole occlusion, coupled with increases in size of regions of myocardial hypoxia (Control = 22.0% vs. Microspheres = 42.2%).
Conclusions: Cardiac mechanical performance is very sensitive to arteriolar blockade, but metabolite switching from fatty acid to glucose utilisation may also support cardiac function in regions of declining PO_2.
General significance: Preserving functional capillary supply may be critical for maintenance of cardiac function when metabolic flexibility is lost, as in diabetes.

1. Introduction

The heart has a high and unremitting demand for energy derived largely from oxidation of lipids, with a lesser contribution from glucose [1]. Lipid oxidation requires an adequate supply of oxygenated blood to facilitate maximum ATP production from the fewest molecules of substrate. However, complete oxidation of glucose yields more ATP per molecule of oxygen consumed, and is hence more efficient where oxygen availability may be limiting. Indeed, inhibition of fatty acid β-oxidation with trimetazidine led to increased glucose oxidation, coupled with increases in cardiac mechanical work despite no changes in oxygen consumption for both rat [2] and human hearts [3], suggesting more efficient ATP production. Given the relationship between oxygen consumption and coronary flow [4], substrate selection by the working heart may be dictated by the availability of oxygen and/or coronary flow. Hence, conditions such as compensated cardiac hypertrophy that are characterised by regions of tissue ischaemia within the myocardium [5] exhibit increased glucose oxidation and decreased fatty acid β-oxidation [6]. Further compromise to oxygen supply, e.g. during decompensated cardiac failure and ischaemic injury, leads to an increased reliance on glycolysis, enabling production of ATP without requiring oxygen [7]. This is inefficient in terms of substrate use, characterised by the heart transitioning from being a net importer of lactate to the synthesis and export of excess lactate [8]. Therefore,

Abbreviations: CD, capillary density; HR, heart rate; KH, Krebs Henseleit buffer; LAD, left anterior descending coronary artery; NN, nearest neighbour; PO_2, partial pressure of oxygen; RPP, rate-pressure product; SAN, sino-atrial node.

* Corresponding author. Tel.: +44 113 3430685.
E-mail address: d.hauton@leeds.ac.uk (D. Hauton).

http://dx.doi.org/10.1016/j.bbagen.2014.12.014
0304-4165/

capillary supply of oxygenated blood is critically important to the optimisation of myocardial ATP production. This may be of particular consequence following rarefaction of capillary supply to the heart, as occurs in conditions such as diabetes [9] and hypertension [10].

Recent experiments document the heterogeneous nature of blood flow distribution within the adult heart *in vivo*, suggesting that not all capillaries are continuously perfused. Indeed, periods of reduced myocardial flow may be a normal cardiac phenomenon, largely controlled by arteriolar autoregulation [11]. Other factors may influence oxygen delivery beyond arteriolar dilatation, and hence perfusion. For example, diabetes led to a thickening of myocyte capillary basement membranes in both rats [12] and humans [13] with resulting increases in capillary diffusion distance presenting physical barriers to oxygen exchange [14]. Furthermore, increases in cardiac muscle fibre diameter (as typified by cardiac hypertrophy) lead to increased intercapillary distance [15] and reduced cardiac performance [16]. In addition, heterogeneity of capillary supply may be an independent variable in limiting oxygen delivery [17], with increases in heterogeneity associated with greater severity of cardiac impairment [18].

Decreased perfusion of cardiac muscle and impaired coronary flow reserve may predict mortality in humans [10] with microvascular diseases such as diabetes [11], as a close correlation between oxygen demand and capillary distribution normally matches delivery with utilisation [19]. We therefore postulated that if microvascular units (an individual arteriole and its associated capillaries supplied downstream) are responsible for local provision of oxygen to the myocardium, loss of functional capillaries by occlusion of individual arterioles would decrease work performed by the heart, and hence decreased total metabolism, without altering the balance between lipid and glucose metabolism for the remaining muscle fibres as no 'spillover' of oxygen into adjacent capillary domains may occur. Conversely, if diffusion of oxygen over wider distances supports metabolism in neighbouring fibres/capillary domains then metabolism will be altered to improve the efficiency of ATP production through 'metabolic flexibility'. This response involves switching of substrate use to efficiently exploit the prevailing oxygen supply, exemplified by a decrease in fatty acid oxidation and increased reliance on glucose metabolism.

The isolated crystalloid-perfused heart offers the best method to investigate the effects of altered functional capillary supply in the heart. This overcomes autoregulation of coronary arterioles by perfusing with a high oxygen partial pressure yet low content medium [20,21] enabling the contribution of individual, maximally-dilated arterioles to contractile performance and regional metabolism in the myocardium to be investigated. Exploiting microspheres, we selectively occluded arterioles in the perfused heart from naive rats. Histological analysis was used to discriminate between patent capillaries and those with microsphere-occluded flow to estimate degree of occlusion, and correlate this with myocardial function and metabolism as well as calculated tissue oxygenation.

2. Materials & methods

2.1. Materials

^{3}H-[9,10]-oleic acid and [U-^{14}C] glucose were purchased from Amersham Biosciences (Chalfont, UK); polystyrene microspheres (15 μm mean diameter) from Molecular Probes (Eugene, Oregon, USA); fatty acid-free bovine albumin and all buffer salts from Sigma (Poole, UK); fluorescein-labelled lectin was purchased from Vector laboratories (UK), Cy3-labelled anti-α-smooth muscle actin antibody from Sigma (Poole, UK). All solvents were ANALAR grade and purchased from Fisher Scientific (Loughborough, UK). Ventricular balloons were constructed 'in house' using Saran Wrap polythene film.

2.2. Methods

2.2.1. Animal maintenance

All experiments were carried out in accordance with the UK Home Office, Animal Scientific Procedures Act (1986) and were approved by the University of Birmingham local ethics committee. Male Wistar rats (265 ± 11 g) were maintained and housed at 22 °C 12 h light/12 hr dark with *ad libitum* access to food (Lillico RM3, rat chow) and water throughout the experiment. A total of 35 untreated rats were used.

2.2.2. Tissue isolation and heart perfusion

Hearts were prepared from fed rats as outlined previously [22]. Briefly, anaesthesia was induced with halothane (4% in oxygen) and following thoracotomy hearts were excised and the aorta cannulated (16G cannula), then perfused in retrograde fashion [23]. A small flexible non-elastic balloon was inserted into the left atrium through the mitral valve and into the left ventricle. This fluid-filled balloon was attached to a fine plastic catheter and connected to a pressure transducer and a graduated syringe (0–1000 μl: Hamilton, Nevada, USA). Hearts were maintained at 37 °C and perfused at a constant pressure (100 cm H_2O) with a Krebs–Henseleit crystalloid medium (KH) supplemented with glucose (10 mM) and $CaCl_2$ (1.3 mM) gassed with oxygen/CO_2 (95:5). Developed pressure (peak—end diastolic pressure) was measured following isovolumic contraction and recorded to computer using a digital interface (AD Instruments, Chalgrove, Oxford, UK). The initial balloon volume was adjusted until measured end-diastolic pressure was 0 mm Hg and the systolic pressure was recorded. Balloon volume was increased in incremental steps (50 μl) until the peak systolic pressure developed exceeded 200 mm Hg and developed pressure was recorded in real time. Coronary flow was estimated from timed collections of a known volume of perfusate and expressed as volume/time/unit mass of cardiac tissue. Preliminary experiments were undertaken to establish a single concentration of microspheres needed to produce a significant decrease in cardiac work. For selected experiments, 1×10^5–1×10^7 microspheres (mean diameter 15 ± 0.2 μm, appropriate to block terminal arterioles) were suspended in KH-bovine albumin solution (4% *w*/*v*) and were infused directly into the aortic perfusion line. Given the retrograde nature of this perfusion technique microspheres were infused directly into the coronary circulation. A period of stabilisation (10 min) followed prior to repetition of the performance estimation (Supplemental Fig. 1A). Ventricular performance was calculated off-line as detailed previously [23].

For separate perfusions quantifying 'steady-state' functional parameters of the heart, hearts were perfused as detailed above with intraventricular balloon incorporated in the LV [23]. The LV balloon volume was adjusted to give an end-diastolic pressure (EDP) = 10 mm Hg until EDP was stable (typically 5 min). Estimates of systolic pressure, developed pressure and heart rate were calculated and performance was calculated as above [23].

2.2.3. Perfused working heart

Working hearts were perfused as previously described [22]. Atrial filling pressure was fixed at 10 cm H_2O with an afterload fixed at 100 cm H_2O. Hearts were perfused with KH, together with glucose (10 mM supplemented with U-^{14}C-labelled glucose 0.185 MBq/perfusion) and palmitic acid (0.4 mM pre-bound to bovine albumin + ^{3}H palmitic acid 5.55 MBq/perfusion). All hearts were unpaced. Metabolism was estimated from timed collection of perfusate and effluent gases (see below) for 45 min to quantify utilisation of glucose and palmitate (Supplemental Fig. 1B). The heart was then returned to perfusion in Langendorff mode and microspheres in KH infused directly into the aortic line and the heart retrograde perfused for a further 3 min to ensure transfer of microspheres into the coronary circulation. Hearts were then returned to 'working mode' and perfused through the left atrium at fixed pre- and afterload, as above. Timed collections of both perfusate and effluent gases were then continued for a further 45 min

(Supplemental Fig. 1B). At termination of the experiment LV free wall was dissected and frozen (see below) to determine the degree of arteriole occlusion with microspheres. Hearts that did not maintain contractile activity throughout both phases of the protocol were excluded from estimates of metabolism.

2.2.4. Estimates of oxygen consumption

For selected experiments myocardial oxygen extraction was estimated from real-time arterial and coronary venous oxygen partial pressure using a 'flow-through' Microx TX2-AOT oxygen microsensor (Presens, Precision Sensing-GmbH, Germany). A 2-point calibration was undertaken (oxygen-saturated KH buffer and oxygen-free KH buffer) prior to the experiment. Oxygen content of the KH perfusate was calculated with reference to the Bunsen solubility coefficient for oxygen (22.7 μl O_2/ml at 1 atm) and oxygen extraction was calculated from the coronary flow/unit cardiac mass. Cardiac efficiency was calculated as rate-pressure product (mm Hg/min/g heart)/oxygen consumption (μmoles O_2/min/g heart) to estimate work generated/unit oxygen consumed (mm Hg/μmole O_2).

2.2.5. Quantitation of perfusate tritiated water

For selected experiments, metabolism of palmitate was estimated from quantitation of ^3H_2O production, as previously described [22]. Briefly, aliquots of perfusate (1.0 ml) were extracted with chloroform: methanol (2:1) and metabolism was estimated in the aqueous fraction by scintillation counting. Metabolism was calculated with reference to the specific activity at the start of the experiment.

2.2.6. Glucose metabolism

For selected hearts perfusate glucose was supplemented with U-^{14}C-labelled glucose (as above). Effluent gases were collected from a gas-tight perfusion apparatus into ethanolamine/ethylene glycol (2:1) solution [24] and samples of perfusate were recovered to estimate the liberation of ^{14}C-labelled CO_2 as CO_2 or bicarbonate, as previously detailed [22].

2.2.7. Lactate flux

Aliquots of perfusate were combined with perchloric acid (PCA; 0.6 N) to deproteinise the sample and stored for later analysis. For neutralised PCA-treated perfusate samples lactate was estimated enzymatically, following the conversion of lactate to pyruvate and quantifying NADH absorbance at 340 nm [25]. Rates of lactate accumulation were estimated from timed collections of perfusate, and linear regression analysis of lactate synthesis used to estimate the rate of lactate production.

2.2.8. Estimates of acetyl-CoA synthesis

To give an estimate of 'total metabolism', rates of acetyl-CoA synthesis were calculated from the rates of metabolism for glucose and palmitate measured from the perfusate. Briefly, estimates were based on the assumption that metabolism of 1 mole of glucose by complete metabolism yields 2 moles acetyl-CoA, and complete metabolism of 1 mole palmitate yields 9 moles acetyl-CoA [26].

2.2.9. Perfusate lactate dehydrogenase (LDH) activity

Ischemia-induced damage to the myocardium was estimated from perfusate LDH activity. Briefly, aliquots of perfusate were recovered and frozen immediately before addition of microspheres and 45 min following microsphere infusion to quantify ischemic injury. LDH activity was subsequently measured [5] in the presence of excess NAD (10 mg/ml final concentration), using lactate (5 mM final concentration) as a substrate. Rates of NADH production were calculated with reference to the molar extinction coefficient for NADH (340 nm = 6220 M^{-1} cm^{-1}) and expressed with reference to cardiac mass.

2.2.10. Capillary density

Tissues were mounted onto cork disks (22 mm: R.A. Lamb, Eastbourne, East Sussex, UK) in Tissue-Tek OCT compound (Sakura, Torrance, CA) before freezing in liquid nitrogen-cooled isopentane. Cryostat sections (10 μm) were cut and fixed onto glass slides. Capillaries were visualised using fluorescein-labelled *Griffonia simplicifolia* lectin (Vector Laboratories, UK) and arterioles were quantified from Cy3-labelled anti-α-smooth muscle actin antibody using a Ziess Axioskop microscope [27]. Vessel density was quantified from digital images (magnification ×200) in regions of known area for four non-consecutive sections using Image J (NIH) image analysis software. A minimum of six fields were counted per section; three sections for each heart were quantified. Sections were counted at random and the viewer was blinded to the origins of the tissue. Data is expressed as capillary profiles/mm^2 cross-sectional area.

2.2.11. Estimation of arteriolar occlusion

To estimate degree of arteriole occlusion (to correlate with the decrement in performance and metabolism) left ventricle sections were cut from perfused hearts and embedded in OCT before freezing in liquid nitrogen-cooled isopentane. Cryostat sections of left ventricle free wall were air dried, fixed with phosphate-buffered formalin, stained with C3 conjugate-labelled anti-α-smooth muscle actin (C6198, Sigma, UK) and mounted in Vectorshield containing DAPI as nuclear counter stain (Vector Laboratories, UK). From each heart 4 sections not less than 200 μm apart were counted through the vertical thickness of the LV (sampling a total of at least 600 μm). For each section, 4 regions of epicardium and 4 regions of endocardium were counted. DAPI staining allowed for correction for areas containing no myocardium (Supplemental Fig. 3). All sections were counted at low magnification (×100 image). Arterioles and microspheres were counted from the same fields and expressed as percentage occlusion. For each heart the mean of the 4 sections (sampled at 4 different depths of LV) was calculated and this represents the percentage arteriolar occlusion for an individual heart. Hence, for each heart 16 non-consecutive fields of epi- and endocardium were quantified to estimate the degree of arteriolar occlusion.

2.2.12. Visualisation of patent capillaries

For selected hearts at the end of microsphere perfusion FITC-labelled Dextran (MW ~500,000: 20 mg/ml in 4% bovine albumin) was infused into the coronary circulation *via* a 3-way tap inserted into the aortic perfusion, prior to mounting on cork disks in OCT. Coronary perfusion pressure was maintained at 100 cm H_2O throughout. Care was taken not to introduce air bubbles into the coronary circulation. Hearts were intact, apex upper-most and frozen as above. Hearts were cryostat-sectioned (25 μm thickness) in subdued light to prevent photo-bleaching of the FITC-Dextran. Sections were then fixed and counterstained as above with rhodamine-lectin (Vector Laboratories, UK) and viewed under fluorescence microscopy (Ziess Axioskop). Images were taken from the mid-wall of the LV (magnification ×200) and overlaid using Image J to estimate the distribution of patent capillaries. Total capillary supply was visualised with lectin (red) whilst patent capillaries, possessing flow after infusion of microspheres, contained FITC-Dextran (green).

2.3. Oxygen diffusion calculations

Binary images of total and patent capillary supply for identical regions were taken (above). The shortest distance between adjacent capillaries was calculated by Delaunay triangulation, producing a value for the summed influence of all nearest neighbours [28], to determine the variance in capillary supply in the normal state and following arteriole occlusion with microspheres. Domain area was calculated following Voronoi tessellation of digitised images, to produce non-overlapping polygons centred around an individual capillary, whose boundaries were defined as a point equidistant between two adjacent capillaries, i.e. representing the half-maximal distance between 'nearest

neighbours' [16]. The coefficient of variation was calculated for capillary density, domain area, and nearest neighbour distance (NN) as standard deviation/mean × 100.

Spatial distributions of tissue oxygen tension (PO_2) and consumption rate (MO_2) were generated using a two-dimensional circular region within a cross section of heart muscle tissue. This was modelled as a homogeneous tissue composition, with an array of capillaries of circular cross-section (with radius, $r_{cap} = 2$ μm) supplying O_2 to the tissue with Michaelis–Menten consumption kinetics [51]; O_2 transport within the myocardium was therefore described by the equation

$$\alpha D \nabla^2 p - \frac{M_0 p}{p + p_c} = 0, \quad (1)$$

where p is tissue PO_2, α is tissue O_2 solubility, D is tissue O_2 diffusivity, M_0 is the maximum tissue O_2 demand, and p_c is tissue PO_2 when O_2 consumption is half of the demand. At each capillary–tissue interface, the flux is proportional to the difference in PO_2 across this wall, and was thus described by the boundary condition

$$n \cdot [\alpha D \nabla p] - k\left(p_{cap} - p\right) = 0, \quad (2)$$

where p_{cap} is the transversely averaged intercapillary PO_2, k is the mass transfer coefficient, and $\boldsymbol{n}$ denotes the outward unit normal vector. Also, at the exterior boundary a no-flux condition was assumed

$$n \cdot [aD \nabla p] = 0, \quad (3)$$

though the analysed region of interest is sufficiently far from the external boundary to ensure insensitivity to the details of the boundary condition. Eqs. ((1)–(3)) were solved to determine tissue PO_2 using the finite element method, implemented using Matlab (The MathWorks Inc., Natick, MA) with a nonlinear solver based on a Gauss–Newton iteration, with adaptive meshing to resolve areas of rapid change in oxygen partial pressures.

In the simulations, we used capillary densities estimated from each tissue cross section (control density = 1661 capillaries/mm^2; occluded density = 1200 capillaries/mm^2) which fixed the physical domain size for a given number of capillaries. As suggested by [21], we also use the following biophysical parameters

$$\alpha = 4.42 \times 10^{-3}\ \text{ml}\ O_2 \cdot 100\ \text{ml}^{-1} \cdot \text{mm}\ \text{Hg}^{-1},$$
$$D = 8.7 \times 10^{-4}\ \text{cm}^2 \cdot \text{min}^{-1}, p_{cap} = 40\ \text{mm}\ \text{Hg},$$
$$k = 5.16 \times 10^{-2}\ \text{ml}\ O_2 \cdot \text{min}^{-1} \cdot \text{cm}^{-2} \cdot \text{mm}\ \text{Hg}^{-1},$$
$$M_0 = 0.2286\ \text{ml}\ O_2 \cdot \text{ml}^{-1} \cdot \text{min}^{-1}, r_{cap} = 2\ \mu\text{m},$$

where a cut-off of $p_c = 0.5$ mm Hg was used to describe regions of tissue hypoxia [29].

2.4. Statistical analysis

As all experiments involved consecutive measurements within the same heart following intervention a paired t-test was used to compare the impact of microsphere infusion on metabolism of the heart pre- and post-arteriole occlusion with microspheres. Data represents mean ± standard deviation. Curve fitting analysis and estimation of mathematical functions were undertaken with appropriate computer software (CurveExpert 1.4-2009). Correlation coefficients were calculated using Spearman's rank method and 'best fit' was estimated assuming a linear relationship, with statistical significance calculated using Student's t-test. $P < 0.05$ was taken to indicate statistical significance.

3. Results

3.1. Histological analysis

Arteriolar density was not significantly different between epicardium and endocardium for perfused hearts (NS, Supplemental Table 1). In these hearts, capillary density of the endocardium was 12% lower than the epicardium ($P < 0.05$, Supplemental Table 1), but the average number of capillaries supplied by one arteriole was similar in epicardium and endocardium of perfused hearts (NS, Supplemental Table 1). Infusing a single dose of microspheres (3×10^5/heart) led to 40% reduction in number of capillaries perfused ($P < 0.001$, Fig. 1A), with the coefficient of variation in myocardial capillary density increasing 20% following microsphere infusion (CV = 19.2% untreated *vs.* 25.8% occluded). Using Voronoi tessellation to estimate capillary domain size showed a 60% increase in supply area ($P < 0.01$; Fig. 1B), coupled with a 20% increase in distance to the nearest capillary neighbour ($P < 0.01$; Fig. 1C).

3.2. Microsphere occlusion and cardiac performance

3.2.1. Langendorff hearts

Arteriolar occlusion with microspheres led to a decline in cardiac performance (estimated as RPP) for Langendorff-perfused hearts with intraventricular balloon. The curvilinear decrease in HR was steepest when occlusion was >30% (Supplemental Fig. 2A). RPP showed a linear decline with increasing occlusion, with 50% decrease following 30% occlusion of arterioles ($R^2 = 0.820$; Supplemental Fig. 2B). Furthermore, cardiac RPP showed a positive correlation with coronary flow ($R^2 = 0.821$; Supplemental Fig. 2C). Estimates of cardiac pressure–volume relationships showed diastolic performance were preserved in perfused hearts, with reductions only in developed pressures manifest, as decreased systolic performance for balloon volumes <350 μl ($P < 0.01$; Supplemental Fig. 2D). For balloon volumes >350 μl systolic pressures were preserved. RPP declined 50% ($P < 0.001$) following infusion of a fixed dose of microspheres (Supplemental Fig. 2E). To confirm maximal dilatation of coronary vessels in hearts perfused with KH-buffer, sodium nitroprusside (SNP-100 μM final concentration) was infused and no change to mean coronary flow was noted (control = 7.5 ± 1.0 ml/min/gm *vs.* SNP = 7.4 ± 1.12 ml/min/gm, NS).

3.2.2. Perfused working heart

Increasing arteriolar occlusion with microspheres led to an exponential decline in mechanical performance of the perfused working heart, with a 50% decline in RPP noted for 10% arteriolar occlusion (Fig. 2A). Infusion of microspheres led to a decline in coronary flow with a corresponding decrease in oxygen consumption by the heart ($r^2 = 0.888$: Fig. 2B). However, for cardiac efficiency (cardiac work/unit oxygen consumed) an inverse correlation was noted, implying that efficiency of the myocardium increased following decreases in oxygen consumption ($r^2 = -0.879$: Fig. 2C). Prior to infusion of microspheres, cardiac output was preserved for the initial 40 min of the perfusion period (Supplemental Fig. 3). Following infusion of microspheres cardiac output (CO) decreased 60% at 45 min ($P < 0.001$; Supplemental Fig. 4) and continued to decline further for the remainder of the perfusion period. This decline fell to 20% of control values but was not significantly different from CO at 45 min (NS; Supplemental Fig. 4). A fixed dose of microspheres added to Langendorff-perfused hearts (3×10^5 microspheres/heart) led to a 30% decline in mean RPP ($P < 0.001$; Fig. 3A) and a 40% decline in mean oxygen extraction ($P < 0.001$; Fig. 3B). However, following estimation of cardiac efficiency, infusion of microspheres increased the efficiency of oxygen consumption for the myocardium by 25% ($P < 0.01$; Fig. 3C).

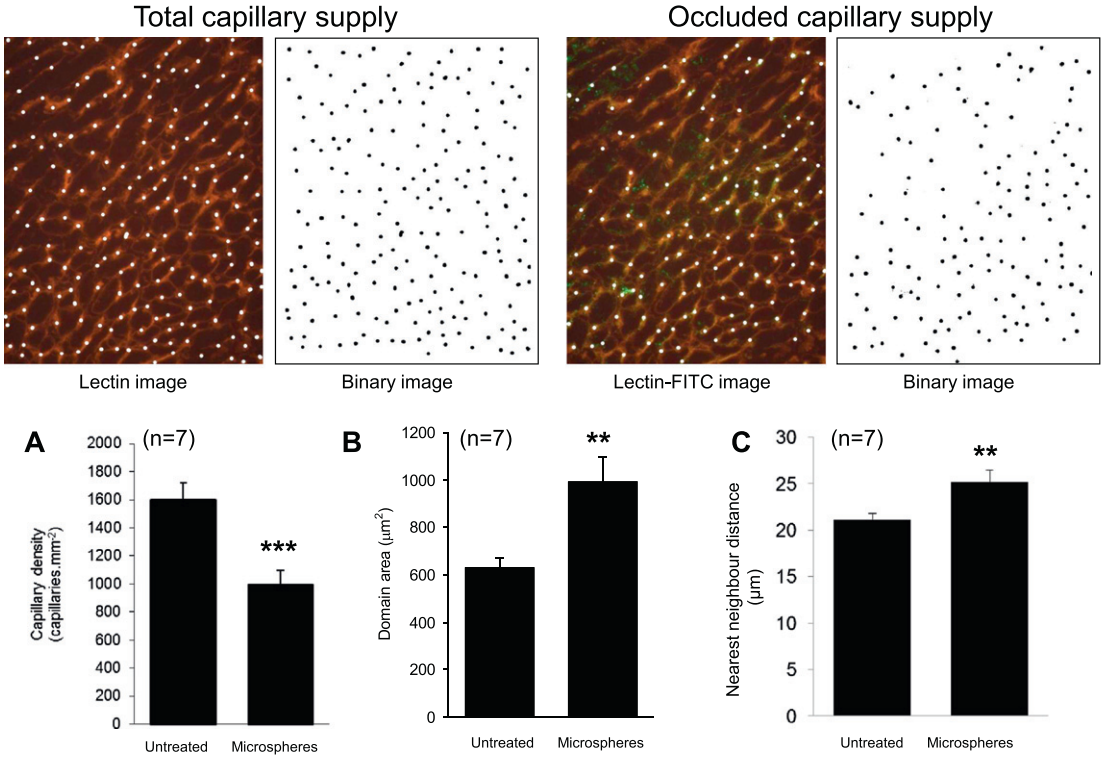

Fig. 1. Histological estimates of total capillary supply and patent capillaries following infusion of 3×10^5 microspheres. Total capillary supply was estimated by rhodamine-labelled lectin-staining of capillaries (red colour). Patent capillaries following microsphere infusion were estimated by inclusion of FITC-labelled dextran (green colour) to highlight only those capillaries possessing flow. Heterogeneity of capillary supply within the same heart was estimated from coefficient of variation for analysis of different regions of LV free wall from an individual heart. Images represent 384 μm × 304 μm of myocardium, thus encompassing 0.116 mm^2. Data represents mean ± SD (n = 7 non-consecutive sections isolated for a single heart). Statistical significance indicated as effect of microsphere infusion ** $P < 0.01$, *** $P < 0.001$.

3.3. Rates of metabolism

For perfused hearts, microsphere infusion decreased cardiac palmitate oxidation rates by 50% ($P < 0.001$, Fig. 4A) and increased glucose oxidation rates by 25% ($P < 0.01$, Fig. 4B). In addition, infusion of microspheres decreased lactate flux to <10% of that for untreated hearts ($P < 0.001$; Fig. 4C).

3.4. Estimated rate of acetyl-CoA production

For control hearts, infusion of a fixed dose of microspheres decreased acetyl-CoA synthesis rates by 30% ($P < 0.001$; Fig. 5A). Estimates of differential substrate utilisation in perfused hearts indicated that 67% of total ATP was obtained from palmitate, 33% obtained from glucose oxidation (Fig. 5B); following infusion of microspheres, the source of acetyl-CoA was calculated as 45% derived from palmitate, the remainder from glucose (all $P < 0.001$, Fig. 5B).

3.5. Arteriolar occlusion and performance of the working heart

Microspheres were distributed throughout the left ventricle homogeneously, providing ~20% occlusion of available arterioles throughout, with no difference between endocardium and epicardium (NS; Supplemental Fig. 4). Since performing differing degrees of cardiac work requires appropriate levels of ATP production, the work performed by each heart was normalised by calculating the metabolic index (MI = substrate utilisation per unit time / unit work performed / unit time) to provide estimates of metabolism undertaken to support a defined quantity of work for fixed time period (Fig. 6). For these normal hearts palmitate MI remained unchanged until RPP had fallen to about 5% of maximum values (Fig. 6), indicating that for a given unit of work equivalent amounts of palmitate underwent β-oxidation, despite an overall decline in total cardiac work. This subsequently increased steeply with further declining work (Fig. 6). For glucose oxidation, however, MI was unchanged until RPP reached approximately 10,000 mm Hg/min, thereafter describing a linear increase with decreasing workload (Fig. 6). Despite occlusion of arterioles with microspheres no increase in perfusate lactate dehydrogenase activities was noting suggesting limited ischemic injury to cardiomyocytes (NS; Supplemental Fig. 5).

3.6. Effects of microsphere occlusion on calculated oxygen diffusion distance

Calculated myocardial PO_2 was sensitive to occlusion of arterioles leading to a decrease in oxygen consumption (control = 16.6 ± 7.2 ml/100 ml · min *vs.* microsphere occluded = 12.4 ± 9.0 ml/100 ml · min; Fig. 7), and an increase in the fractional area of hypoxic regions (control = 22.0% hypoxia *vs.* microsphere occluded = 42.2%; Fig. 7). With a recalculation to include the contribution from myoglobin, oxygen consumption was calculated to be: control 16.7 ± 7.1 ml/100 ml · min (Maximum 22.6, Minimum 3.67×10^{-6}); microsphere occluded 12.5 ± 8.9 ml/100 ml min (Maximum 22.6, Minimum 7.58×10^{-7}). Myoglobin had insignificant contribution to lowering tissue hypoxia.

4. Discussion

The preservation of myocardial arteriole supply is essential for maintenance of cardiac performance, and we demonstrate that progressive occlusion with microspheres led to a decline in cardiac work. We also show that modest degrees of arteriole occlusion (20%) led to a doubling of capillary domain area despite only increasing measured distances

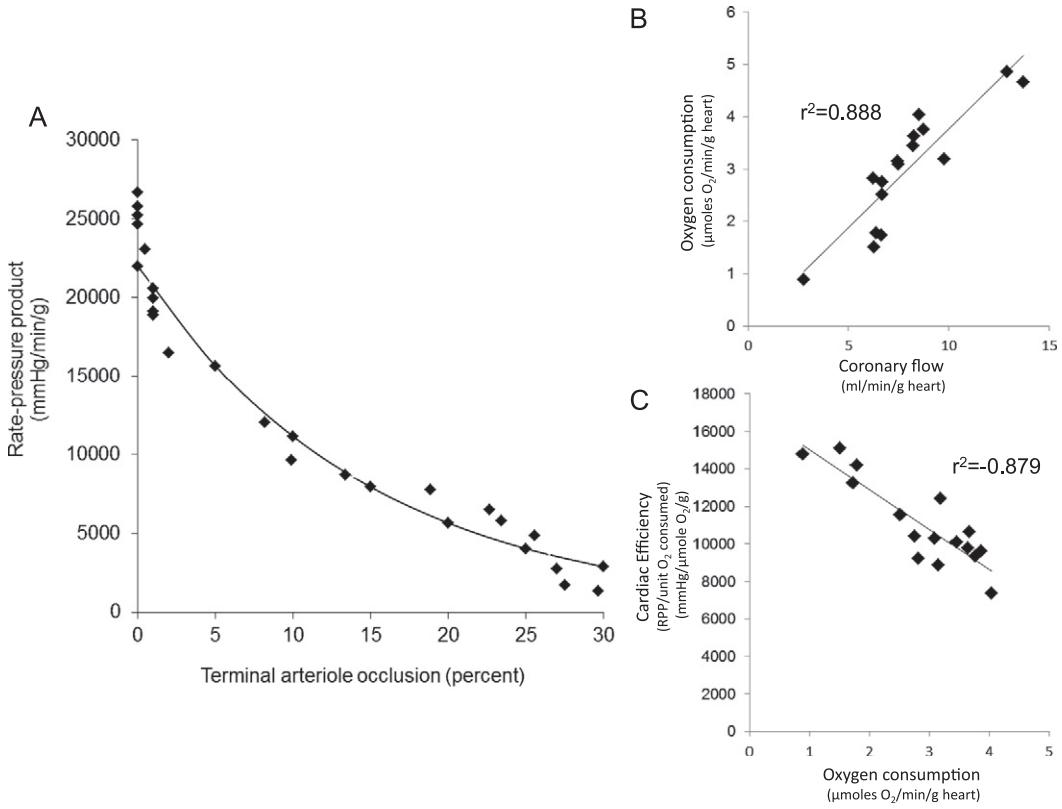

Fig. 2. Effect of microsphere infusion on the mechanical performance of the perfused rat heart. Declining cardiac work with increasing arteriole occlusion in the working heart ($n = 10$ hearts) (A) Effect of declining coronary flow on cardiac oxygen consumption in Langendorff hearts ($n = 8$ hearts) (B) and effects of declining oxygen consumption on cardiac efficiency in Langendorff hearts ($n = 8$ hearts) (C). Perfusates were supplemented with glucose (5 mM) and palmitate (0.4 mM) pre-bound to albumin (1% w/v). The coefficient of determination (r^2) is shown for linear relationships.

between 'nearest neighbour' capillaries by 20%. We also show that normal hearts demonstrate some metabolic plasticity to the regional tissue hypoxia, manifest as a transition from palmitate oxidation to glucose oxidation. This suggests that preservation of capillary supply may be critical to cardiac performance but also that the flexibility to switch between different metabolic substrates, and the subsequent overlap in nutrient supply between adjacent capillaries, may help sustain contractile performance of the remaining viable myocardium. We speculate that the stimulus for this switch is declining myocardial PO_2. We present evidence to support this hypothesis as microsphere occlusion of arterioles led to both a decline in cardiac work and oxygen consumption, while the efficiency of oxygen use (work done per unit oxygen consumed) increased, supporting the switching of substrate utilisation to glucose to improve rates of ATP synthesis for the available oxygen supply.

4.1. Oxygen kinetics

We demonstrate that for the isolated heart, arteriole occlusion by microspheres led to decreased cardiac work coupled with a decrease in oxygen consumption and a theoretical difference in tissue PO_2. Furthermore, this is characterised by an increase in both the size of the calculated regions of hypoxia and an increase in the heterogeneity of capillary domains. This increased heterogeneity in capillary supply accompanies a decline in cardiac performance and a shift in metabolism,

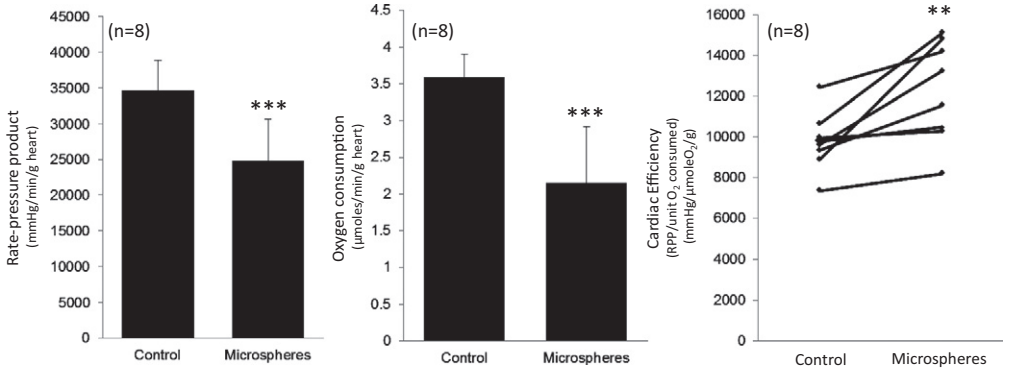

Fig. 3. Effect of a single dose of microspheres infused into Langendorff-perfused rat hearts on rate-pressure product (A), oxygen consumption (B) and cardiac efficiency (C). Hearts were perfused at constant coronary perfusion pressure (100 cm H_2O) and oxygen consumption estimated in real-time by continuous estimation of arterial-venous difference. Data represents mean ± SD ($n = 8$ hearts). Statistical significance indicated as effect of microsphere infusion ** $P < 0.01$, *** $P < 0.001$.

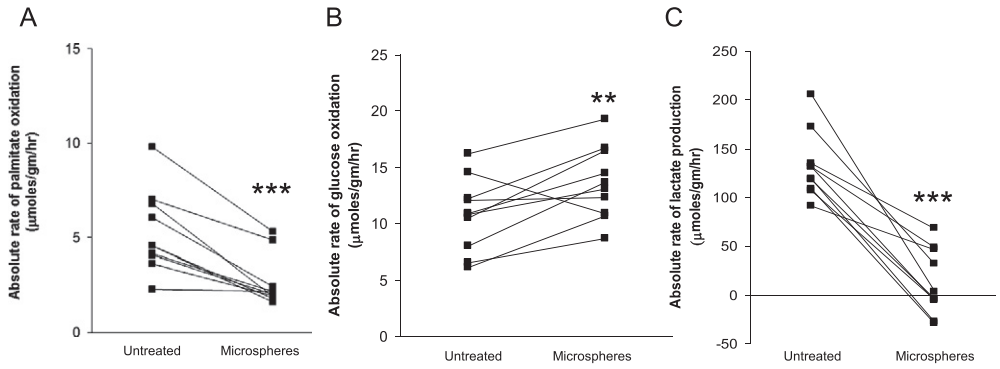

Fig. 4. Absolute rates of metabolism of palmitate (A), glucose (B) and lactate (C) for perfused, working hearts before and after microsphere infusion. Data represents mean ± SD ($n = 10$ hearts). Statistical significance indicated as effect of microsphere infusion ** $P < 0.01$, *** $P < 0.001$.

favouring increases in efficiency of oxygen consumption (greater glucose oxidation). Together, these observations suggest that one determinant for substrate selection may be the efficiency of ATP production within mitochondria, utilising the available oxygen. Recent experiments suggest that the mean mitochondrial PO_2 for Langendorff-perfused hearts is ~25 mm Hg, yet the major fraction of mitochondria are ~5 mm Hg [30], suggesting that our calculated values likely reflect PO_2 in the intact perfused heart. Furthermore, acute declines in mitochondrial PO_2 (10–13 mm Hg) did not decrease the mitochondrial respiration rate, implying that this threshold is sufficient to support oxidative metabolism [31]. Indeed, previous observations suggest that oxidative phosphorylation requires similar oxygen tensions (12 mm Hg) [32,33]. Interestingly, isolated mitochondria show peak oxygen consumption rates at 1.5 mm Hg yet demonstrate a $P_{50} = 0.4$ mm Hg, suggesting that despite arteriole occlusion by microspheres and loss of functional capillary supply, significant regions of the myocardium maintain some level of oxidative metabolism [34]. Mathematical models predict that oxygenation of the crystalloid-perfused rat heart is only adequate at high coronary flow rates (>10 ml/min/g) [21], equivalent to the current observations prior to infusion of microspheres, indicating that we likely generate regions of hypoxia within the myocardium following infusion of microspheres. While cardiac tissue PO_2 declined distal to the site of microsphere injection into the pig coronary circulation, this was sensitive to microsphere size, with 15 μm microspheres (trapped in the terminal arterioles) decreasing tissue PO_2, whilst 10 μm microspheres (trapped within individual capillaries) had no effect [35]. This implies that both decreased oxygen transport and also increased minimum diffusion distances for oxygen following infusion of the larger microspheres. These observations support the validity of using microspheres to occlude terminal arterioles, and also suggest that occlusion of individual capillaries with the smaller microspheres contributes little to changing oxygen delivery [35] because loss of available surface area for gaseous exchange from one capillary is minute as a proportion of the total. In addition, individual capillary blockages may be readily compensated by anastomoses. However, for occluded terminal arterioles only collateral circulation connecting the different microvascular units of blocked and unblocked arterioles are potentially relevant. Moreover, each such anastomosis will supply less than one capillary's perfusate flux to a blocked arteriole's microvascular unit. Thus, whilst we have not considered anastomoses/collateral circulation in detail, and indeed measuring their contribution to redistribution of flow in the heart is difficult using the analytical approach outlined here, such effects are likely to be subordinate, for instance if the capillary bed downstream of an arteriole is sufficiently large.

4.2. Cardiac performance

Our initial experiments showed that heart rate reduction required a profound degree of arteriole occlusion and might reflect differences in coronary flow between the sino-atrial node (SAN) and ventricular muscle, or the relative insensitivity of SAN to this form of acute hypoxic insult [36]. We used this mechanistic information to quantify the numbers of microspheres needed to produce a modest degree of arteriole occlusion, affecting inotropy alone, as a direct relationship between heart rate and oxygen consumption is seen [37]. Interestingly, cardiac mechanical range and diastolic performance were not altered following infusion of microspheres, supporting the notion that, acutely, the greatest impact is manifest on energy-dependent systolic function.

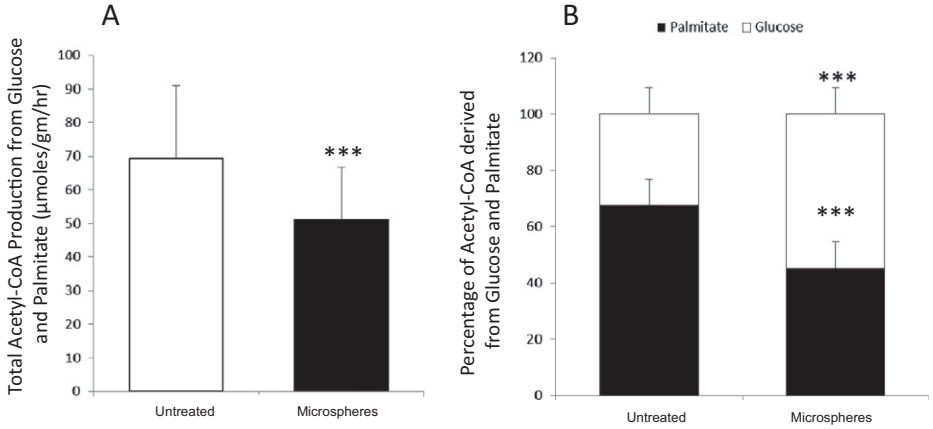

Fig. 5. Estimated rates of acetyl-CoA production before and after microsphere infusion. Rates of acetyl-CoA synthesis following arteriole occlusion (A) and the proportion of acetyl-CoA synthesised from exogenous palmitate and glucose (B). Rates of acetyl-CoA synthesis were estimated with reference to the amounts of palmitate and glucose metabolised and theoretical maximum rates of acetyl-CoA synthesis were calculated. Data represents mean ± SD ($n = 10$ hearts). Statistical significance indicated as effect of microsphere infusion *** $P < 0.001$.

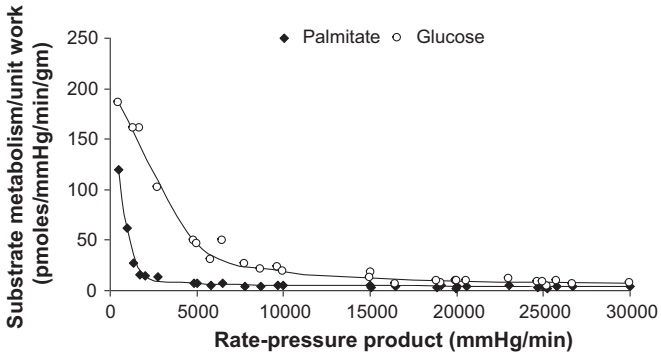

Fig. 6. Rates of metabolism of palmitate and glucose corrected for changes in cardiac work. Curves indicate the extent of the coupling of metabolism for glucose and palmitate with mechanical work for perfused hearts at varying degrees of arteriole occlusion. Metabolic index was calculated as (absolute metabolism/g heart)/rate-pressure product for both glucose and palmitate to correct for the decline in cardiac performance with increasing arteriole occlusion, in order to determine whether the 'metabolism per unit cardiac work' was preserved throughout the range of cardiac performance ($n = 15$ hearts).

Of interest is the gradual, curvilinear decline for RPP with increasing degree of arteriole occlusion, suggesting that we have maintained electrical conductivity among cardiomyocytes. A striking observation is that this model of 'global, moderate-flow ischaemia' induced by microspheres appears more detrimental to cardiac mechanical performance than coronary artery ligation: occluding 10% of arterioles with microspheres led to a 50% reduction in RPP implying a high degree of sensitivity for mechanical work to changes in coronary perfusion. By contrast, LAD ligation in rats to produce an infarct of 50% of the LV free wall yielded only a 10% decrease in cardiac mechanical performance [38]. This may reflect the limited contribution from spillover into adjacent capillary domains. As a consequence small, non-contractile regions of myocardium, produced following microsphere infusion, may yield an increase in muscle tension through an inability to release actin-myosin cross-bridges as a consequence of declining ATP levels. This may increase local internal work and decrease contractile efficiency. However, for the LAD-ligated heart sufficient myocardium may remain unaffected to maintain adequate cardiac work, while regional loss of electrical conductivity may decrease the contractile contribution to ATP consumption. Interestingly, we also note no increase in perfusate lactate dehydrogenase activities following microsphere infusion (Supplemental Fig. 5) possibly indicating the impairment of electrical coupling within the myocardium rather than direct ischemic injury to cardiomyocytes as may be anticipated following, for example, LAD ligation.

4.3. Cardiac metabolism

Normal hearts display substrate flexibility, switching from palmitate to glucose metabolism following arteriole occlusion. We speculate that this reflects 'spillover' in terms of O_2 supply between adjacent capillary

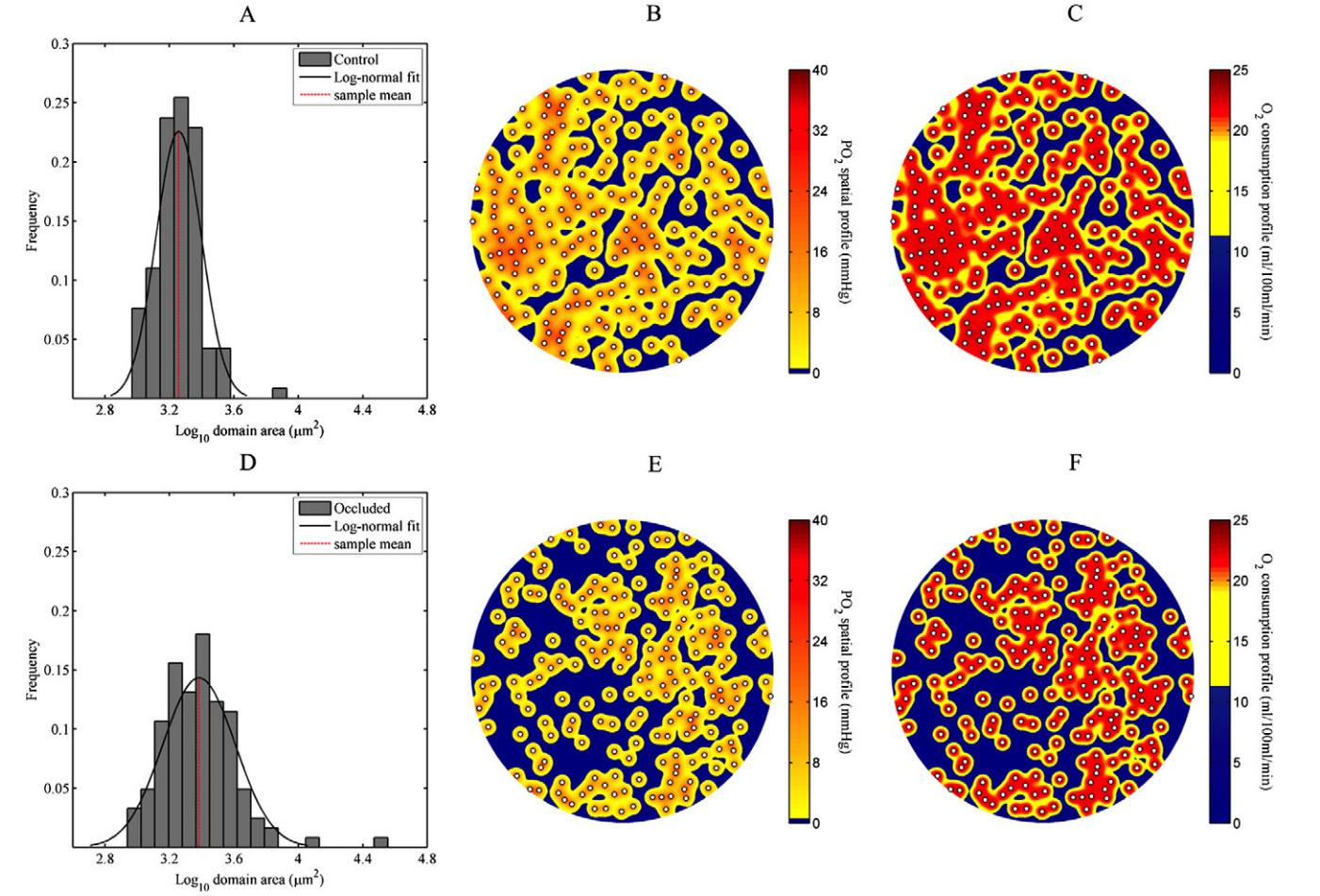

Fig. 7. Variation in capillary domain distribution of control and occluded samples of rat myocardium (A & D). Noting the logarithmic normal distribution of capillary domains, capillary domain areas after arteriolar occlusion increased by 72.2% in this sample with mean values of $\log_{10}$ domain area 3.26 ± 0.14 μm^2 for control *vs.* 3.38 ± 0.22 μm^2 for occluded. Predicted spatial profiles of tissue oxygen tension (B & E) and consumption rate (C & F) show heterogeneity in tissue PO_2 across sections of myocardium before (A,B,C) and after (D,E,F) arteriolar occlusion of control perfused working rat hearts. Representative images documenting both total and patent capillary supply (Fig. 1) were digitised and finite element computations were applied in conjunction with estimates of the diffusivity of oxygen from capillaries to the surrounding myocardium to computationally predict tissue PO_2.

domains sufficient to support glucose oxidation (but not fatty acid oxidation). However, this may represent an increase in work done by segments of normally-perfused myocardium adjacent to regions for which arteriole supply was occluded with microspheres. A 'mild-global ischaemia' model, with coronary flow and cardiac work rates similar to those achieved in the current study, demonstrated preserved rates of fatty acid oxidation and modest reductions in cardiac efficiency during a 40% reduction in coronary flow [26], suggesting a marked reduction of coupling between O_2 consumption and mechanical work. This differs from the current study that demonstrated regional hypoxia and areas of normal perfusion in adjacent regions, thus facilitating the potential for 'spillover' of oxygen. Furthermore, glycolysis may also contribute limited ATP to support cardiac mechanical performance without the consumption of oxygen, thus helping to increase the calculated cardiac efficiency. We cannot exclude the possibility that for the declining coronary perfusion pressure of the working heart following microsphere infusion, occlusion of some arterioles may actually improve perfusion of the remaining arterioles, supporting improved performance of these regions. However, given the high partial pressure and low oxygen content in the perfusate we anticipate maximum dilatation of arterioles, abolishing any local autoregulation of perfusion [20,21], as demonstrated following addition of SNP to the perfusate.

Utilisation of ATP within the heart may be linked to two separate phenomena: maintenance of cardiomyocyte viability and the support of mechanical performance. The reduced estimates for acetyl-CoA synthesis (and hence ATP production) following microsphere infusion are likely a consequence of less mechanical work carried out by the heart. Indeed, our evidence suggests that for the perfused heart as much as one-third of the ATP production is required to maintain viability of cardiomyocytes, even when not contributing to contractile work. When normalised (μmoles metabolism/unit RPP) palmitate oxidation is tightly coupled to cardiac work, and for the current protocol this most likely represents the decline in ATP synthesis as a consequence of decreased O_2 delivery limiting the work done by the heart [39]. This suggests close coupling of oxidative phosphorylation, and a high degree of mitochondrial efficiency. As oxygen is the terminal electron acceptor in oxidative phosphorylation such a relationship was anticipated, given that estimates of [^{3}H]palmitate metabolism are calculated from the production of tritiated water. However, no such direct coupling with glucose metabolism exists. As the synthesis of CO_2 is not exclusively the result of oxidative phosphorylation, from [^{14}C]glucose we may estimate increases in metabolism that produces reducing equivalents (NADH & $FADH_2$) that may yield electrons not producing ATP. In effect, at low workloads glucose metabolism may increase the proton gradient across the inner mitochondrial membrane, although this effect is likely to be modest. Alternatively, increased glucose metabolism at very low workloads may also reflect maintenance of metabolism by cells that are adequately perfused yet poorly coupled electrically. Indeed, previous experiments show that hypoxia led to loss of contractile activity in papillary muscle through loss of the intracellular potassium gradient from cardiomyocytes [40], although this was better maintained with an adequate supply of glucose [41].

4.4. Experimental limitations

Our observations are made with a high partial pressure, low-oxygen content perfusion medium [20] and very high coronary flow rates. Oxygen delivery for the blood-perfused heart may be less sensitive to modest changes to coronary flow [42], despite lower rates, as supply is uncoupled from flow rate [43]. However, previous studies modelling the spatial patterns of capillary supply for human hearts suggest similar oxygen supply (domain) areas to those we measured for the untreated rat heart [16]. Furthermore, following microsphere occlusion a decrease in the regularity of functional capillary spacing is noted (increased coefficient of variation), with increases in domain areas similar to that for patients with ischaemic cardiomyopathy [16,18]. This heterogeneity of capillary supply may leave regions of poorly-oxygenated, non-contractile myocardium contributing to a decrease in mechanical performance and increased internal work for the heart. Previous experiments postulate diffusion of oxygen from other elements of the vasculature (arterioles) [44]; however given the very high flow rates in perfused hearts coupled with the short length of arterioles we predict that diffusion will be almost entirely through the capillary network [45].

As glycogen contributes significantly to glucose turnover in aerobic conditions [46,47], and these small stores are anticipated to last only short periods during ischaemic periods, they probably contribute little to maintaining cardiac performance [48] under the current experimental conditions. Moreover, in the absence of arteriole perfusion-O_2 supply to adjacent tissue, glycogen will make a modest and rapidly declining contribution to overall ATP synthesis. The use of labelled glucose throughout the perfusion period means that ^{14}C-glucose incorporated into glycogen prior to microsphere infusion may subsequently be utilised in the post-occlusion phase, although previous studies also show that this contribution will be small [49].

The oxygen diffusion modelling was undertaken using images from perfused hearts and we therefore cannot exclude changes to architecture of the heart caused by tissue oedema. However, care was taken to minimise this effect by using untreated and microsphere-infused samples that had been perfused for the same (short) duration and are therefore representative of the experiment.

5. Conclusions

Graded loss of arteriole supply led to a reduction in both coronary flow and cardiac work. Metabolism was also decreased as a consequence of arteriole occlusion and the heart demonstrated a capacity to switch between substrates, from palmitate to glucose, to improve both the efficiency of oxygen consumption and sustain cardiac work. Our data suggests that the decline in performance noted for the heart in chronic diabetes may not be solely metabolic in origin but could result from capillary rarefaction and microvascular disease, secondary consequences of diabetes, that lead to a regional inadequacy in oxygenation of the myocardium. Diabetic metabolic restrictions would further limit compensatory cardiac responses to reduced PO_2. This may be of relevance for the diabetic myocardium, given the increased consumption of oxygen to fuel both basal metabolism and excitation–contraction coupling [50].

Acknowledgements

The authors wish to thank the University of Birmingham Research Development Committee for supporting this work. A. A. Al-Shammari is supported by a scholarship from the Department of Mathematics, Kuwait University, Kuwait (FD/SB/FA/UG432).

Appendix A. Supplementary data

Supplementary data to this article can be found online at http://dx.doi.org/10.1016/j.bbagen.2014.12.014.

References

[1] W.C. Stanley, F.A. Recchia, G.D. Lopaschuk, Myocardial substrate metabolism in the normal and failing heart, Physiol. Rev. 85 (2005) 1093–1129.
[2] G.D. Lopaschuk, R. Barr, P.D. Thomas, J.R. Dyck, Beneficial effects of trimetazidine in ex vivo working ischemic hearts are due to stimulation of glucose oxidation secondary to inhibition of long-chain 3-ketoacyl coenzyme a thiolase, Circ. Res. 93 (2003) e33–e37.
[3] H. Tuunanen, E. Engblom, A. Naum, K. Någren, M. Scheinin, B. Hesse, K.E. Juhani Airaksinen, P. Nuutila, P. Iozzo, H. Ukkonen, L.H. Opie, J. Knuuti, Trimetazidine, a metabolic modulator, has cardiac and extracardiac benefits in idiopathic dilated cardiomyopathy, Circulation 118 (2008) 1250–1258.
[4] M.A. Djikman, J.W. Heslinga, P. Sipkema, N. Westerhof, Perfusion-induced changes in cardiac O_2 consumption and contractility are based on different mechanisms, Am. J. Physiol. 271 (1996) H984–H989.

[5] J.F. Ashruf, C. Ince, H.A. Bruining, Regional ischemia in hypertrophic langendorff-perfused rat hearts, Am. J. Physiol. 277 (1999) H1532–H1539.
[6] A. Akki, K. Smith, A.M.L. Seymour, Compensated cardiac hypertrophy is characterised by a decline in palmitate oxidation, Mol. Cell. Biochem. 311 (2008) 215–224.
[7] M.F. Allard, R.B. Wambolt, S.L. Longnus, M. Grist, C.P. Lydell, H.L. Parsons, B. Rodrigues, J.L. Hall, W.C. Stanley, G.P. Bondy, Hypertrophied hearts are less responsive to the metabolic and functional effects of insulin, Am J. Physiol. 279 (2000) E487–E493.
[8] R.K. Evans, D.D. Schwartz, L.B. Gladden, Effect of myocardial volume overload and heart failure on lactate transport into isolated cardiac myocytes, J. Appl. Physiol. 94 (2003) 1169–1176.
[9] O.P. Pitkänen, P. Nuutila, O.T. Raitakari, T. Rönnemaa, P.J. Koskinen, H. Lida, T.J. Lehtimäki, H.K. Laine, T. Takala, J.S. Viikari, J. Knuuti, Coronary flow reserve is reduced in young men with IDDM, Diabetes 47 (1998) 248–254.
[10] D.S. Marks, S. Gudapeti, L.M. Prisant, B. Weir, C. diDonato-Gonzalez, J.L. Waller, J.L. Houghton, Mortality in patients with microvascular disease, J. Clin. Hypertens. 6 (2004) 304–309.
[11] T. Matsumoto, H. Tachibana, T. Asano, M. Takemoto, Y. Ogasawara, K. Umetani, F. Kajiya, Pattern differences between distributions of microregional myocardial flows in crystalloid- and blood-perfused rat hearts, Am. J. Physiol. 286 (2004) H1331–H1338.
[12] L. Okruhlicova, N. Tribulova, P. Weismann, R. Sotnikova, Ultrastructure and histochemistry of rat myocardial capillary endothelial cells in response to diabetes and hypertension, Cell Res. 15 (2005) 532–538.
[13] V.W. Fischer, H.B. Barner, L.S. Larose, Pathomorphologic aspects of muscular tissue in diabetes mellitus, Hum. Pathol. 15 (1984) 1127–1136.
[14] R.A. Malik, P.G. Newrick, A.K. Sharma, A. Jennings, A.K. Ah-See, T.M. Mayhew, J. Jakubowski, A.J. Boulton, J.D. Ward, Microangiopathy in human diabetic neuropathy: relationship between capillary abnormalities and the severity of neuropathy, Diabetologia 32 (1989) 92–102.
[15] L. Henquell, C.L. Odoroff, C.R. Honig, Intercapillary distance and capillary reserve in hypertrophied rat hearts beating *in situ*, Circ. Res. 41 (1977) 400–408.
[16] R. Karch, F. Neumann, R. Ullrich, J. Neumüller, B.K. Podesser, M. Neumann, W. Schreiner, The spatial pattern of coronary capillaries in patients with dilated, ischemic or inflammatory cardiomyopathy, Cardiovasc. Pathol. 14 (2005) 135–144.
[17] Z. Turek, K. Rakuŝan, Lognormal distribution of intercapillary distance in normal and hypertrophic rat heart as estimated by the method of concentric circles: its effects on tissue oxygenation, Pflugers Arch. 391 (1981) 17–21.
[18] R. Karch, F. Neumann, R. Ullrich, G. Heinze, J. Neumüller, B.K. Podesser, M. Neumann, Methods from the theory of random heterogeneous media for quantifying myocardial morphology in normal and dilated hearts, Ann. Biomed. Eng. 38 (2010) 308–318.
[19] S. Egginton, E. Gaffney, Tissue capillary supply—it's quality not quantity that counts! Exp. Physiol. 95 (2010) 971–979.
[20] K.A. Schenkman, Cardiac performance as a function of intracellular oxygen tension in buffer-perfused hearts, Am. J. Physiol. 281 (2001) H2463–H2472.
[21] D.A. Beard, K. Schenkman, O. Feigl, Myocardial oxygenation in isolated hearts predicted by an anatomically realistic microvascular transport model, Am. J. Physiol. 285 (2003) H1826–H1836.
[22] D. Hauton, M.J. Bennett, R.D. Evans, Utilisation of triacylglycerol and non-esterified fatty acid by the working rat heart: myocardial lipid substrate preference, Biochim. Biophys. Acta 1533 (2001) 99–109.
[23] D. Hauton, G.M. Caldwell, Cardiac lipoprotein lipase activity in the hypertrophied heart may be regulated by fatty acid flux, Biochim. Biophys. Acta 1821 (2012) 627–636.
[24] H. Jeffay, J. Alvarez, Liquid scintillation counting of carbon-14. Use of ethanolamine-ethylene glycol monoethylether-toluene, Anal. Chem. 33 (1961) 612–615.
[25] J.F. Neville Jr., R.L. Gelder, Modified enzymatic methods for the determination of L-(+)-lactic and pyruvic acids in blood, Am. J. Clin. Pathol. 55 (1971) 152–158.
[26] C.D. Folmes, D. Sowah, A.S. Clanachan, G.D. Lopaschuk, High rates of residual fatty acid oxidation during mild ischemia decrease cardiac work and efficiency, J. Mol. Cell. Cardiol. 47 (2009) 142–148.
[27] J.L. Williams, D. Cartland, A. Hussain, S. Egginton, A differential role for nitric oxide in two forms of physiological angiogenesis in mouse, J. Physiol. 570 (2006) 445–454.
[28] S. Egginton, H.F. Ross, Influence of muscle phenotype on local capillary supply, Adv. Exp. Med. Biol. 247 (1989) 281–291.
[29] D.F. Wilson, W.L. Rumsey, T.J. Green, J.M. Vanderkooi, The oxygen dependence of mitochondrial oxidative phosphorylation measured by a new optical method for measuring oxygen concentration, J. Biol. Chem. 263 (1988) 2712–2718.
[30] E.G. Mik, C. Ince, O. Eerbeek, A. Heinen, J. Stap, B. Hooibrink, C.A. Schumacher, G.M. Balestra, T. Johannes, J.F. Beek, A.F. Nieuwenhuis, P. van Horssen, J.A. Spaan, C.J. Zuurbier, Mitochondrial oxygen tension within the heart, J. Mol. Cell. Cardiol. 46 (2009) 943–951.
[31] C.A. Di Maria, M.A. Bogyevitch, D.J. McKitrick, L.F. Arnolda, L.C. Hool, P.G. Arthur, Changes in oxygen tension affect cardiac mitochondrial respiration rate via changes in the rate of mitochondrial hydrogen peroxide production, J. Mol. Cell. Cardiol. 47 (2009) 49–56.
[32] W.L. Rumsey, C. Schlosser, E.M. Nuutinen, M. Robiollo, D.F. Wilson, Cellular energetic and oxygen dependence of respiration in cardiac myocytes isolated from adult rat, J. Biol. Chem. 265 (1990) 15392–15399.
[33] D.L. Hoffman, J.D. Salter, P.S. Brookes, Response of mitochondrial reactive oxygen species generation to steady state oxygen tension: implications for hypoxic signalling, Am. J. Physiol. 292 (2007) H101–H108.
[34] E. Gnaiger, G. Méndez, S.C. Hand, High phosphorylation efficiency and depression of uncoupled respiration in mitochondria under hypoxia, Proc. Natl. Acad. Sci. U. S. A. 97 (2000) 11080–11085.
[35] B. Hiebl, C. Mrowietz, S. Lee, S. Braune, M. Knaut, A. Lendlein, R.P. Franke, F. Jung, Influence of polymeric microspheres on myocardial oxygen partial pressure in the beating heart of pigs, Microvasc. Res. 82 (2011) 52–57.
[36] K. Fukuzaki, T. Sato, T. Miki, S. Seino, H. Nakaya, Role of sarcolemmal ATP-sensitive K+ channels in the regulation of sinoatrial node automaticity: an evaluation using Kir6.2-deficient mice, J. Physiol. 586 (2008) 2767–2778.
[37] K. Clarke, R.J. Willis, Energy metabolism and contractile function in the rat heart during graded, isovolumic perfusion using 31P nuclear magnetic resonance spectroscopy, J. Mol. Cell. Cardiol. 19 (1987) 1153–1160.
[38] D.S. Burley, G.F. Baxter, B-type natriuretic peptide at early reperfusion limits infarct size in the rat isolated heart, Basic Res. Cardiol. 102 (2007) 529–541.
[39] C. Nakajima-Takenaka, G.X. Zhang, K. Obata, K. Tohne, H. Matsuyoshi, Y. Nagai, A. Nishiyama, M. Takaki, Left ventricular function of isoproterenol-induced hypertrophied rat hearts perfused with blood: mechanical work and energetics, Am. J. Physiol. 297 (2009) H1736–H1743.
[40] A.A. Wilde, A.G. Kléber, The combined effects of hypoxia, high K+ and acidosis on the intracellular sodium activity and resting potential in guinea pig papillary muscle, Circ. Res. 58 (1986) 249–256.
[41] S.M. Yabek, R. Kato, B.N. Singh, Effects of hypoxia on the cellular electrical activity of adult and neonatal canine ventricular myocardium, Pediatr. Res. 19 (1985) 1263–1267.
[42] B.J. Friedman, O.Y. Grinberg, S.A. Grinberg, H.M. Swartz, Myocardial oxygen tension in isolated erythrocyte-perfused rat hearts and comparison with crystalloid media, J. Mol. Cell. Cardiol. 29 (1997) 2855–2858.
[43] M. Radisic, W. Deen, R. Langer, G. Vunjak-Novakovic, Mathematical model of oxygen distribution in engineered cardiac tissue with parallel channel array perfused with culture medium containing oxygen carriers, Am. J. Physiol. 288 (2005) H1278–H1289.
[44] A.S. Popel, R.N. Pittman, M.L. Ellsworth, Rate of oxygen loss from arterioles is an order of magnitude higher than expected, Am. J. Physiol. 253 (1989) H921–H924.
[45] C.R. Honig, T.E. Gayeski, Precapillary O_2 loss and arteriovenous O_2 diffusion shunt are below limit of detection in myocardium, Adv. Exp. Med. Biol. 247 (1989) 591–599.
[46] H. Fraser, G.D. Lopaschuk, A.S. Clanachan, Assessment of glycogen turnover in aerobic, ischemic and reperfused working rat hearts, Am. J. Physiol. 275 (1998) H1533–H1541.
[47] S.L. Henning, R.B. Wambolt, B.O. Schönekess, G.D. Lopaschuk, M.F. Allard, Contribution of glycogen to aerobic myocardial glucose utilisation, Circulation 93 (1996) 1549–1555.
[48] B. Cosyns, S. Droogmans, S. Nernot, C. Degaillier, C. Garbar, C. Weytjens, B. Roosens, D. Schoors, T. Lahoutte, P.R. Franken, G. Van Camp, Effect of streptozotocin-indiced diabetes on myocardial blood flow reserve assessed by myocardial contrast echocardiography in rats, Cardiovasc. Diabetol. 7 (2008) 26.
[49] D. Hauton, Does metformin increase cardiac lipoprotein lipase? Metab. Clin. Exp. 60 (2011) 32–42.
[50] N. Boardman, A.D. Hafstad, T.S. Larsen, D.L. Severson, E. Aasum, Increased O_2 cost of basal metabolism and excitation–contraction coupling in hearts from type 2 diabetic mice, Am. J. Physiol. 296 (2009) H1373–H1379.
[51] A.A. Al-Shammari, E.A. Gaffney, S. Egginton, Modelling capillary oxygen supply capacity in mixed muscles: capillary domains revisited, J. Theor. Biol. 356 (2014) 47–61.